Journal Pre-proofs

The dynamic catalysis of Ga/ZSM-5 catalysts for propane-CO_2 coupling conversion to aromatics and syngas

Yonggui Song, Zhong-Pan Hu, Haohao Feng, Enze Chen, Le Lv, Yimo Wu, Zhen Liu, Yong Jiang, Xiaozhi Su, Feifei Xu, Mingchang Zhu, Jingfeng Han, Yingxu Wei, Svetlana Mintova, Zhongmin Liu

PII: S2095-4956(24)00411-X
DOI: https://doi.org/10.1016/j.jechem.2024.06.009
Reference: JECHEM 3920

To appear in: *Journal of Energy Chemistry*

Received Date: 23 April 2024
Revised Date: 29 May 2024
Accepted Date: 6 June 2024

Please cite this article as: Y. Song, Z-P. Hu, H. Feng, E. Chen, L. Lv, Y. Wu, Z. Liu, Y. Jiang, X. Su, F. Xu, M. Zhu, J. Han, Y. Wei, S. Mintova, Z. Liu, The dynamic catalysis of Ga/ZSM-5 catalysts for propane-CO_2 coupling conversion to aromatics and syngas, *Journal of Energy Chemistry* (2024), doi: https://doi.org/10.1016/j.jechem.2024.06.009

The dynamic catalysis of Ga/ZSM-5 catalysts for propane-CO_2 coupling conversion to aromatics and syngas

Yonggui Song[a,b], Zhong-Pan Hu[b], Haohao Feng[b], Enze Chen[b], Le Lv[b], Yimo Wu[b], Zhen Liu[c], Yong Jiang[c], Xiaozhi Su[c], Feifei Xu[b], Mingchang Zhu[a,*], Jingfeng Han[b,*], Yingxu Wei[b], Svetlana Mintova[d], Zhongmin Liu[b]

[a] *The Key Laboratory of the Inorganic Molecule-Based Chemistry of Liaoning Province and Laboratory of Coordination Chemistry, Shenyang University of Chemical Technology, Shenyang 110142, Liaoning, China*

[b] *National Engineering Research Center of Lower-Carbon Catalysis Technology, Dalian National Laboratory for Clean Energy, iChEM (Collaborative Innovation Center of Chemistry for Energy Materials), Dalian Institute of Chemical Physics, Chinese Academy of Sciences, Dalian 116023, Liaoning, China*

[c] *Shanghai Advanced Research Institute, Chinese Academy of Sciences, Shanghai 201203, China*

[d] *Normandie University, Laboratory of Catalysis and Spectrochemistry (LCS), ENSICAEN, UNICAEN, CNRS, Caen 14050, France*

*Corresponding authors.

Email addresses: mczhu@syuct.edu.cn *(M. Zhu)*; jfhan@dicp.ac.cn *(J. Han)*

ABSTRACT: Alkane coupling with CO_2 by metal-containing zeolites catalysis is found to be a promising way to produce aromatics and syngas in recent years, but the real active sites and the role of CO_2 are still unclear owing to the quick evolution of the metallic active sites and the complex reaction processes including direct propane aromatization, CO_2 hydrogenation, reverse water-gas shift reaction, and propane-CO_2 coupling aromatization. Herein, Ga/ZSM-5 catalysts were constructd to study the dynamic evolution of the metallic active sites and the role of CO_2 during the propane and CO_2 coupling reaction. After optimizing the reaction conditions, a notable

propane conversion rate of 97.9% and an impressive aromatics selectivity of 80.6% in hydrocarbons can be achieved at the conditions of 550 °C and CO_2/C_3H_8 of 4. $^{13}CO_2$ isotope experiments illustrate that C-atoms of CO_2 can enter into CO (86.5%) and aromatics (10.8%) during the propane-CO_2 coupling reaction process. In situ XANES and FTIR spectroscopies at 550 °C and H_2/C_3H_8 atmosphere reveal that GaO_x species can be gradually dispersed into $[GaH_2]^+/[GaH]^{2+}$ on the Brønsted acid sites of ZSM-5 zeolite during H_2 and/or C_3H_8 treatment, which are the real active sites for propane-CO_2 coupling conversion. In situ CO_2-FTIR experiments demonstrate that the $[GaH_2]^+/[GaH]^{2+}$ species can react with CO_2 and accelerate the propane and CO_2 coupling process. This work not only presents a cost-effective avenue for CO_2 utilization, but also contributes to the active site design for improved alkane and CO_2 activation in coupling reaction system.

KEYWORDS: Carbon dioxide; Propane aromatization; Ga/ZSM-5; Gallium hydride; Spectroscopy

1. Introduction

Propane stands out as a vital component in both conventional and unconventional natural gases, including shale gas [1]. The advent of hydraulic fracturing technology has facilitated the extensive extraction of shale gas in recent years [2]. Moreover, alkanes emerge as significant byproducts in processes such as petroleum refining, coal bed gas production, and steel manufacturing [3]. Maximizing the utilization of these alkanes becomes imperative. Benzene, toluene, and xylene (BTX) constitute crucial chemical raw materials extensively employed in pharmaceuticals, chemicals, materials science, and other fields [4]. Their primary sources encompass catalytic reforming of naphtha and gasoline cracking [5]. However, traditional methods for BTX production entail high costs and energy consumption. Given the escalating global demand for BTX, the conversion of propane, the principal component of shale gas, into high-value-added products emerges as a compelling alternative, fostering the efficient use of shale gas and heightened BTX production [6]. This has garnered attention from both academia and industry [7,8]. Simultaneously, carbon dioxide (CO_2) emerges as an abundant, cost-effective, non-toxic, and recyclable C1 resource, prominently featured as a major chemical and petrochemical raw material in diverse industrial processes [9,10]. The conversion of CO_2 into economically valuable and practically significant products presents a pivotal opportunity for sustainable development [11–14].

CO_2-assisted propane dehydrogenation and aromatization represent a promising method because CO_2 can enhance the aromatization of light alkanes through various mechanisms, exhibiting synergistic effects together with diverse catalysts [15,16]. The

coke transferred from aromatization can be efficiently consumed through the reverse Boudouard reaction with the participation of CO_2, effectively mitigating catalyst deactivation [17]. Additionally, carbon dioxide actively participates in the elimination of H_2 via the reverse water-gas shift (RWGS) reaction [18]. This involvement promotes propane dehydrogenation and aromatization, facilitating the production of more aromatic hydrocarbons through the forward reaction. On the other hand, carbon dioxide, acting as a weak oxidant, plays a crucial role in promoting propane conversion and enhancing selectivity towards aromatic products, and at the same time, the over-oxidation of intermediates is suppressed, thereby optimizing the overall efficiency of the process [19].

ZSM-5 with an MFI type framework structure is characterized by intersecting straight channels with dimensions of 5.3 Å × 5.6 Å and sinusoidal channels with dimensions of 5.1 Å × 5.6 Å, both forming 10-membered ring channels. Due to its inherent acidity, high surface area, high porosity, and thermal stability, ZSM-5 finds widespread application in the chemical and petrochemical industries [20,21]. The cross-channel structure of ZSM-5 plays a crucial role in preventing rapid deactivation of the Brønsted acid sites (BAS) caused by coking, making it an exceptional catalyst for various reactions [22,23]. However, unmodified ZSM-5 catalysts exhibit low activity and aromatic selectivity since the C-H bond of alkane is hard to be dissociated on BAS [24]. To address these challenges, various metal-modified ZSM-5 catalysts and coupling reaction processes have been developed [25,26].

The coupling reactions of CO_2 and alkanes using ZSM-5 have been developed [27–30]. Wei et al. have reported on a coupling system that utilizes CO_2 and butane over HZSM-5, proposing a mechanism that involves methyl-substituted lactones and methyl-substituted cycloalkenones as crucial intermediates [27]. Ren et al. [3] highlighted that on HZSM-5, CO_2 is actively engaged in aromatization by forming oxygen-containing intermediates, including lactones, carboxylic acids, and anhydrides. These intermediates, featuring carbonyl and ester groups, undergo conversion into aromatic hydrocarbon precursors such as olefins, olefins/cycloolefins, or dienes/cyclo-dienes, ultimately leading to the production of aromatics. Guo et al. [31] combined of experimental and DFT theoretical calculations to reveal that introducing zinc into ZSM-5 could effectively suppresses the activation of C-C bond in propane, and minimize undesirable cracking reactions. Furthermore, propene is generated through the activation of the C-H bond of propane, with a barrier of 1.67 eV. By reducing the barriers of the rate-determining steps on Zn/ZSM-5, CO_2 plays a pivotal role in promoting propane activation and aromatization from its olefin product, facilitating the production of aromatics. Structural and electronic property analysis further revealed that the CO_2 alters the hydrogen transfer pathway of the Zn-alkyl species (Zn-C_3H_7 and Zn-C_6H_9), modifies the interaction and strength of bonds in relevant elemental reactions, promotes the transfer of charge from the catalyst to the adsorbate, and stabilizes the transition state of the rate-determining steps. The of P, P-modified Ga/ZSM-5 exhibits improved hydrothermal stability, reduced coke formation, and enhanced production of liquid aromatics through the CO_2-oxidative

dehydrogenation and aromatization reaction [17]. In this process, CO_2 assists in ethylene formation, promoting aromatics production by consuming H_2. Isotope experiments with $^{13}CO_2$ confirmed that aromatics do not contain carbon derived from CO_2.

Ga-modified ZSM-5 zeolite demonstrated superior catalytic performance in the dehydrogenation and aromatization of light alkanes thus considered as a very promising catalyst for alkane aromatization process [17,32–35]. Over the past several decades, extensive research on alkane conversions has been performed on the design of Ga-modified ZSM-5 [36–38]. Ga species loaded on ZSM-5 are weak Lewis acid sites that can promote alkane dehydroaromatication [32]. Gallium species located on Bronsted acid site can transform to GaH_x under H_2 atomsphere [35], but the reverse transformation between GaO_x and GaH_x under working conditions is rarely reported. Gomez et al. proposed tandem reactions of CO_2 reduction and ethane aromatization, providing a theoretical understanding of the role of Ga species through DFT calculations [17]. Although their proposed mechanism is constructive, there is a lack of experimental evidence to support their claims. Alkane conversion, particularly for light alkanes like ethane and propane, often requires harsh conditions such as high temperatures and/or pressures, making it challenging to trace the reaction pathways using in situ spectroscopy. Herein, we investigated the coupling reaction process of CO_2 and propane on Ga/ZSM-5 zeolite. At proper reaction temperature and CO_2/propane ratio, high aromatics selectivity is achieved with the production of syngas and prolonged lifetime. In situ XANES and in situ transmission FTIR were employed to determine the role of gallium hydride and CO_2 in the coupling reaction process, confirming the significance of gallium hydride as an active site for CO_2 conversion. Additionally, ^{13}C isotope tracing experiments were conducted to elucidate the path of CO_2-propane coupling reaction process.

2. Results and discussion

2.1 Properties of Ga/ZSM-5

Ga/ZSM-5 zeolites (Si/Al = 19) with a loading amount of 2.1, 3.95, 6.18, 8.89 wt % were prepared by a commonly used wet impregnation method, followed by oxidation-reduction treatment at 550 °C, which was named as 2%Ga/ZSM-5, 4%Ga/ZSM-5, 6%Ga/ZSM-5,and 9%Ga/ZSM-5 based on the XRF analysis (Table S1). The XRD patterns of the 6%Ga/ZSM-5 and parent ZSM-5 show a series of characteristic peaks at 7-9° and 23-24° (Fig. S1), typical for the MFI structure, suggesting the structure is well preserved after loading Ga species [39]. No characteristic peaks about Ga_2O_3 species can be observed on the Ga/ZSM-5 samples, indicating the Ga species are highly dispersed on the ZSM-5 [40]. The NH_3-TPD results show that the ZSM-5

exhibits two typical desorption peaks at ~230 and 440 °C (Fig. S2), corresponding to NH_3 adsorbed on the weak and strong acid sites of ZSM-5, respectively [41]. After loading with Ga species, the NH_3 desorption temperatures of Ga/ZSM-5 decrease to 210 and 380 °C, respectively. It is notable that the peak intensity of the strong acid sites at 440 °C decreases significantly as the loading amount increases, while the peak corresponding to the weak acid sites at 210 °C decreases slightly, indicating the strong acid sites of ZSM-5 are partially occupied by Ga species [42]. Quantitative analysis of the total acidity shows that the acid amount of the Ga/ZSM-5 catalyst is lower than that of the parent ZSM-5. The acidity analysis utilizing pyridine-FTIR spectroscopy (as shown in Fig. S3) reveals a distinct trend in the concentration of Lewis acid with increasing gallium content. Specifically, the Lewis acid concentration increases steadily as the Ga loading increases, culminating in the highest amount at a loading of 6%. Additionally, upon reaching a Ga loading of 4% or higher, the ratio of Brønsted acid and Lewis acid exhibits minor variations, as detailed in Table S2. Figs. S4–S6 show the SEM images of HZSM-5, 6%Ga/ZSM-5 and the elemental mapping images (Al, Si, and Ga) of 6%Ga/ZSM-5. There is no significant change in the morphology of the zeolite before and after Ga loading, and the Ga species are uniformly distributed on the ZSM-5 zeolite. The H_2-TPR profiles of 6%Ga/ZSM-5 (Fig. S7) present a main H_2 consumption peak at 420 °C and two peaks at 620 and 920 °C, which may be caused by the reduction of different GaO_x species [43].

2.2 CO_2-assisted propane oxidative dehydroaromatization on Ga/ZSM-5 zeolite

Fig. 1, Figs. S8, and S9 show the activities of direct propane dehydroaromatization and propane-CO_2 coupling reaction with different CO_2/C_3H_8 ratios at various reaction temperatures on the Ga/ZSM-5 catalysts. At optimal conditions (550 ℃ and CO_2/C_3H_8 = 4), a high aromatic selectivity of ~80% can be obtained on the 6%Ga/ZSM-5 catalyst. Compared with HZSM-5, the introduction of gallium into the ZSM-5 zeolite results in a gradual increase in propane and CO_2 conversion, accompanied by a dramatic enhancement in aromatics selectivity. This remarkable improvement can be attributed to the critical effect of Lewis acidity arising from gallium modification (Figs. S2 and S3). As depicted in Figs. S8 and S9, the highest propane and CO_2 conversion, as well as the highest aromatics selectivity, are achieved over the 6%Ga/ZSM-5 catalyst. This optimal performance aligns well with the highest acid amount observed for this particular catalyst (Table S2).

It can be seen that the reaction temperature can significantly affect the propane-CO_2 coupling performance (Fig. 1a, b and Tables S3–S5). At the reaction temperature lower than 550 °C, the propane conversion increases with the reaction temperature and both propane and CO_2 conversion are really low, because the CO_2 can be easily

adsorbed onto the Brønsted acid sites of HZSM-5 and Ga species and prevent the adsorption and activation of propane. When the reaction temperature increses to 550 °C, the propane conversion (97.9%) and aromatic selectivity (80.6%) can be improved after introducing CO_2, probably due to the occurrence of reverse water gas shift reaction and the Boudouard reaction at high temperature which eliminates a part of CO_2 (>500 °C). Fig. 1(c and d) show the influcnce of the CO_2/C_3H_8 ratio on the cataltyic performance of Ga/ZSM-5 on propane-CO_2 coupling reaction, showing that CO_2/C_3H_8 = 4 is the optimized ratio. This is probably due to the fact that the CO_2/C_3H_8 ratio of 4 can balance the CO_2 and propane adsorption/activation onto the Ga/ZSM-5 catalyst.

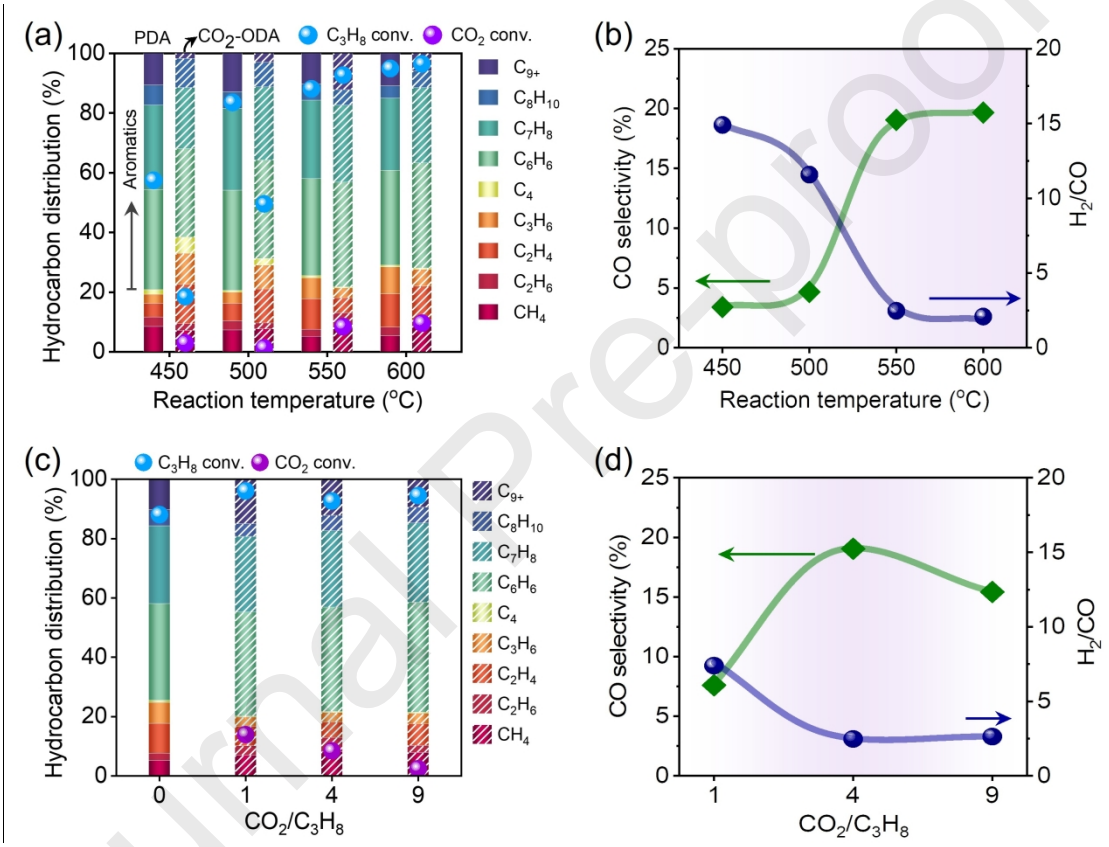

Fig. 1. (a) C_3H_8 and CO_2 conversion, hydrocarbon distribution and (b) CO selectivity and H_2/CO ratio as a function of reaction temperature with a CO_2/C_3H_8 ratio of 4. (c) C_3H_8 and CO_2 conversion, hydrocarbon distribution and (d) CO selectivity and H_2/CO ratio with varied CO_2/C_3H_8 ratio. Reaction conditions: 1 atm, $P_{propane}$ = 0.005 MPa, $WHSV_{propane}$ = 0.6 h^{-1}, time on stream = 1 h.

2.3 The dynamic and reversible state of Ga species under different atmospheres

In situ transmission FTIR was utilized to elucidate the state of Ga/ZSM-5 in H_2 or propane atmosphere. As depicted in Fig. 2(a), the bands at 3584 and 3662 cm^{-1}, associated with the OH vibration of Brønsted acid sites in HZSM-5, concurrently decrease in intensity under H_2 at 550 °C [44]. At the same time, the peaks at 2036 and 2050 cm^{-1} are gradually increased, attributed to the formation of $[GaH_2]^+$ and $[GaH]^{2+}$ species, which could be eliminated by subsequent D_2 exchange. (Fig. 2b and Fig. S10) [45,46]. The decrease of the Brønsted acid sites in HZSM-5 suggests that the reduced Ga species are dispersed on Brønsted acid sites to form a stable structure [47]. A similar phenomenon can be observed under C_3H_8 atmosphere, albeit with lower intensity and a different proportion of gallium hydrides (Fig. 2c and d) [48]. X-ray absorption near-edge structure (XANES) of the Ga K edge of Ga/ZSM-5 under H_2 at 550 °C is presented in Fig. 2(e). With time on stream, the blue shift in the near-edge region can be clearly observed [49]. The subsequent decrease in the white line region is attributed to the deteriorating symmetry of the coordination structure, in good consistent with the FTIR results [50]. The structure of the Ga/ZSM-5 catalyst in an reduction atmosphere is schematically shown in Fig. 2(f), illustrating the GaO_x will be dispersed onto the Brønsted acid sites of HZSM-5 zeolite in H_2/C_3H_8 atmosphere and result in $[GaH_2]^+/[GaH]^{2+}$ species. Upon introducing air into the reduced Ga/ZSM-5 catalyst, the catalyst quickly returned to its initial state (Figs. S11 and S12). This indicates the dynamic and reversible evolution of Ga states and dispersions under different atmospheres.

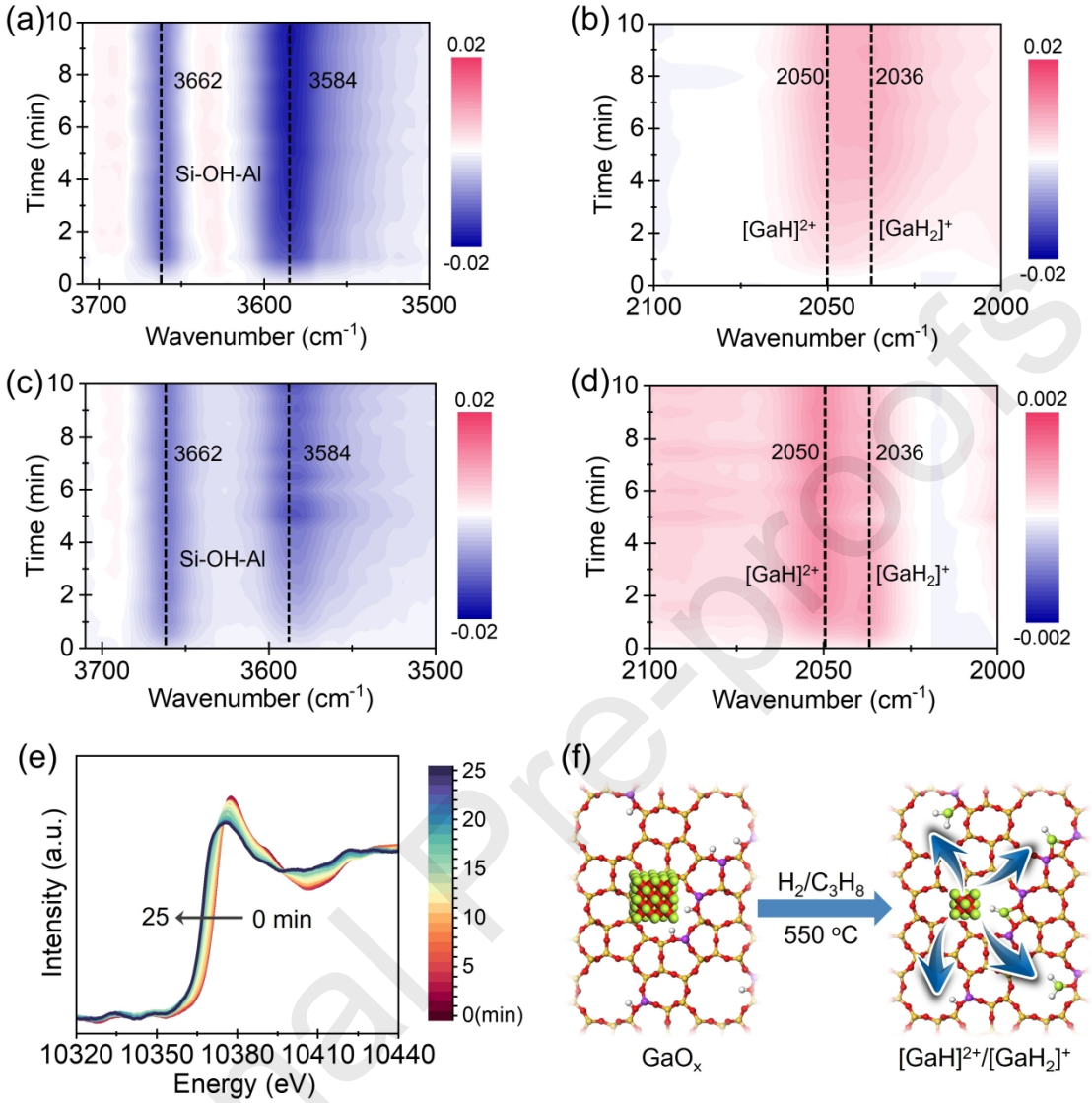

Fig. 2. FTIR spectra of Ga/ZSM-5 catalyst as a function of TOS under (a, b) H_2 and (c, d) C_3H_8 atmosphere at 550 °C. (e) X-ray absorption near-edge structure (XANES) of the K edge of Ga/ZSM-5 in H_2 at 550 °C. (f) The schematic structure of Ga/ZSM-5 in reduction atmosphere.

2.4 The state of the Ga species under coupling reaction condition

In situ transmission FTIR was employed to investigate the C_3H_8-CO_2 co-feeding reaction. As depicted in Fig. 3(a and b), upon introducting of a mixture of CO_2 and C_3H_8, the peaks of $[GaH_2]^+$ at 2033 cm^{-1} and $[GaH]^{2+}$ at 2056 cm^{-1} are appeared, confirming the presence of gallium hydrides in the cofeeding reaction system. With CO_2 coupling, the band at 2082 cm^{-1} attributed to the absorbed CO are appeared,

elucidating the origin of syngas in the coupling reaction [51–53]. In situ XANES was utilized to monitor the oxidation states of gallium sites under working conditions (Fig. 3c). The slight blue shift in the near-edge region of the Ga K edge indicates the formation of GaH_x species, which is in a good agreement with previous results. Fig. 3(d) shows XANES under different atmospheric conditions. The pink dashed line represents the initial state of Ga/ZSM-5, which changes to the deep blue dashed line through hydrogen reduction. After introducing CO_2, Ga is partially oxidized (green and orange dashed lines) by the CO_2. After calicinaiton in air, the spectra will be restored to the initial state (blue dashed line). The results in in good consistented with the FTIR results, suggesting the acid sites and GaH_x are restored to their initial states after air calcination (Figs. S11 and S12).

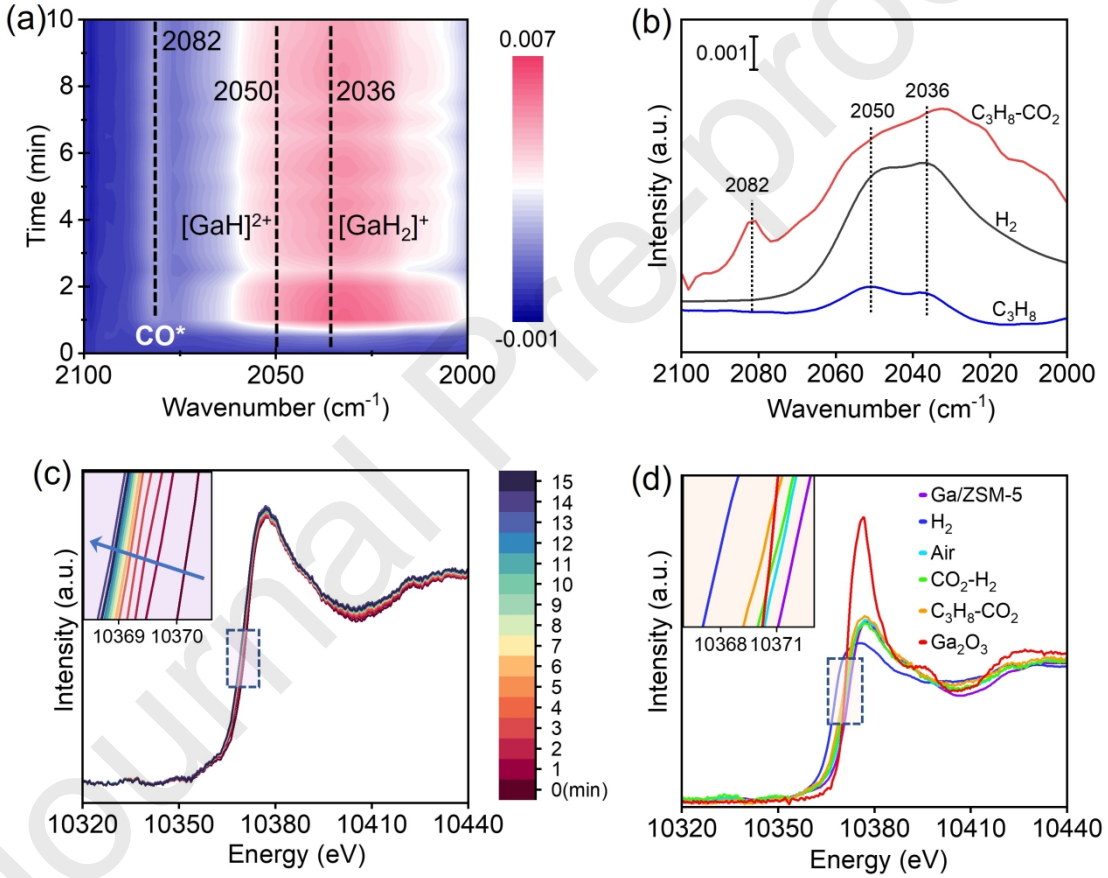

Fig. 3. (a) In situ FTIR spectra of propane-CO_2 coupling reaction over Ga/ZSM-5 as a function of TOS. (b) FTIR spectra of Ga/ZSM-5 under different atmosphere at TOS of 10 min. (c) In situ X-ray absorption near-edge structure (XANES) of propane-CO_2 coupling reaction over Ga/ZSM-5 as a function of TOS. (d) In situ XANES of Ga/ZSM-5 under different atmosphere. The inset in (c) and (d) shows the near-edge region of XANES the K edge of Ga. All spectra were collected at 550 °C.

2.5 CO_2 participation in the coupling reaction pathway

To pinpoint the active sites for CO_2 in the C_3H_8-CO_2 coupling reaction, we explored the reactivity of CO_2 and gallium hydride using an in situ transmission FTIR spectroscopy. As shown in Fig. 4(a), the Ga/ZSM-5 catalyst was initially treated with H_2 for 5 minutes to generate $[GaH_2]^+$ and $[GaH]^{2+}$, followed by Ar purging in the IR cell. The reduced GaH_x species are persisted even after 30 min of Ar sweeping, indicating the remarkable stability of gallium hydrides. Upon changing the purging gas to 20% CO_2/Ar, a fast reduction in gallium hydrides is observed, nearly disappearing within 5 min, accompanied by the emergence of a CO adsorption peak at 2082 cm^{-1} (Fig. 4b). The slight shifts from 2036 to 2039 cm^{-1} for $[GaH_2]^+$ and from 2050 to 2056 cm^{-1} for $[GaH]^{2+}$ may be attributed to the adsorption of CO_2 on the gallium hydrides. These findings unambiguously indicate the activation of CO_2 on reduced Ga species, leading to the formation of CO.

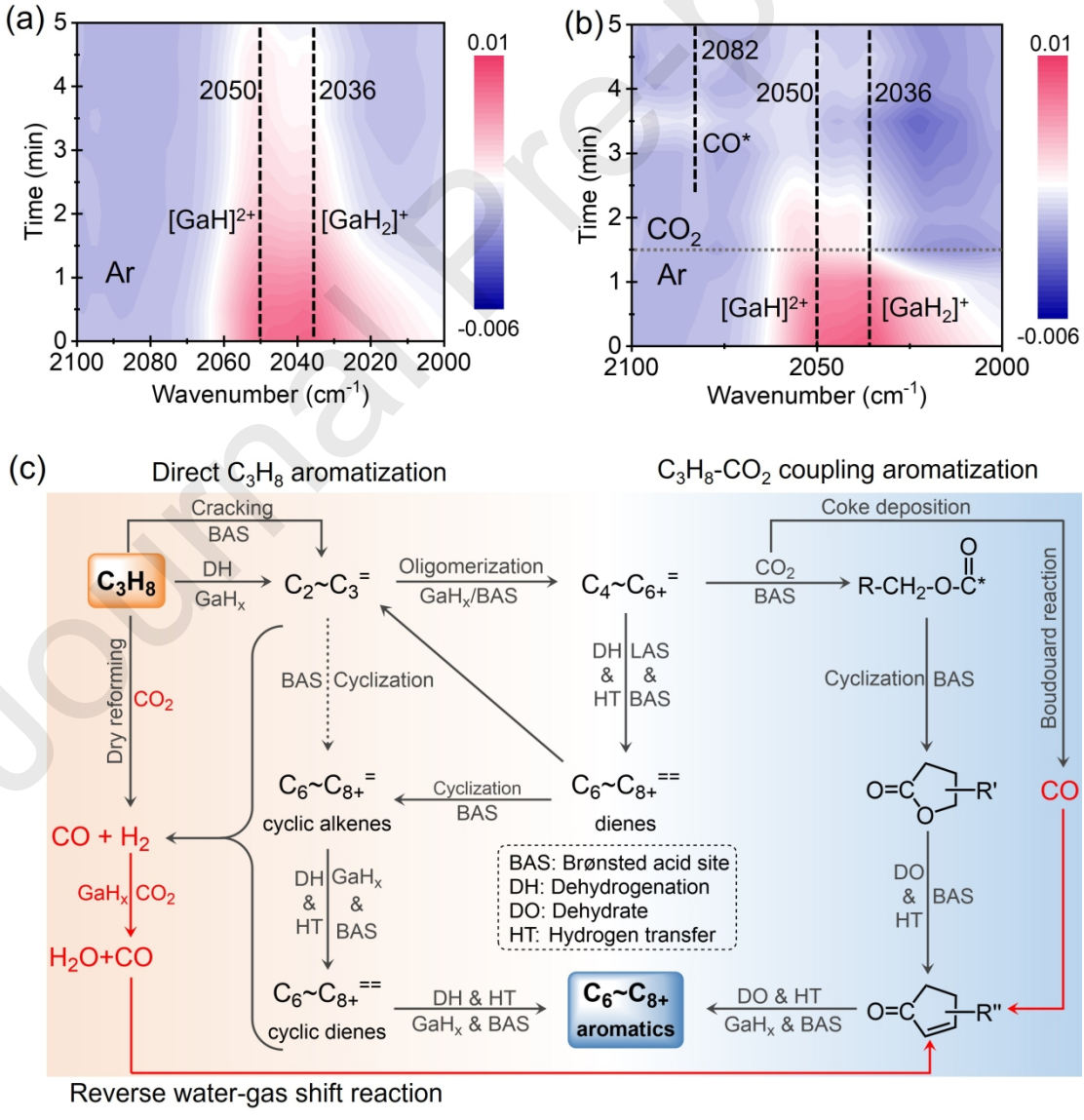

Fig. 4. FTIR spectra of $[GaH]^{2+}$ and $[GaH_2]^{+}$ in Ar (a) and CO_2 (b) atmosphere at 550 °C as a function of time on stream. (c) Schematic illustration of the coupling reaction network of propane and CO_2, including direct propane aromatization (left), CO_2 hydrogenation and reverse water-gas shift reaction (leftdown), dry reforming (leftmost side), Bouduard reaction (rightmost side), and propane-CO_2 coupling aromatization (right).

To trace the footprint of CO_2, we conducted a $^{13}CO_2$ isotope-labeled experiment to investigate the distribution of ^{13}C in the products during the coupling reaction of $^{13}CO_2$ and C_3H_8 (Fig. S13) [54]. It is shown that 86.5% of CO_2 is converted to CO, signifying a substantial involvement of CO_2 in the elimination of hydrogen through the reverse water gas reaction in the coupling process (Fig. 4c). Additionally, 10.8% of CO_2 is entered into aromatics, potentially following the pathway of cyclic lipid intermediates proposed in previous studies on CO_2-coupled alkane conversion (Fig. 4c) [3,19,55]. The equilibrium conversion of Boudouard reaction at various temperatures are calculated by the HSC chemistry 5.0 (Fig. S14). It is notable that the Boudouard reaction is started at ~400 °C. At 550 °C, the equilibrium conversion of CO_2 can be reached to 6.8%, indicating the Boudouard reaction can delay a part of coke at the C_3H_8-CO_2 coupling reaction conditions, leading to the 13.5% CO evolution from ^{12}C-propane. The delayed deactivation rate of Ga/ZSM-5 in C_3H_8-CO_2 coupling reaction also suggests the presence of Boudouard reaction during the C_3H_8-CO_2 coupling reaction (Fig. S15). Furthermore, direct propane dehydroaromatization can be occurred during the coupling reaction process. Stability test shows that a high propane conversion rate of 80% and 5.6% CO_2 conversion rate can be maintained after 5 h time on stream, suggesting the proming utilization of these process in industry.

3. Conclusions

In this work, Ga/ZSM-5 catalysts are prepared by a facile wet-impregnation method to study the dynamic evolution of the Ga species and the role of CO_2 in propane and CO_2 coupling to aromatics and syngas reaction. A series of techniques including XANES, FTIR, XRD, NH_3-TPD, SEM, and H_2-TPR are performed to identify the complex GaO_x species and their evolution on the as-synthesized Ga/ZSM-5 catalysts. The gallium modified ZSM-5 catalysts exhibits a remarkable propane conversion rate of 97.9% with an aromatics selectivity of 80.6% in hydrocarbons at an optimized reaction condition of propane and CO_2 coupling reaction, arising from the introduction of Lewis acid and total acid amount. $^{13}CO_2$ isotope experiments illustrate that C-atoms of CO_2 can enter into CO (86.5%) and aromatics (10.8%) during the coupling reaction process. The dynamic and reversible evolutions of the Ga species

elucidated by in situ spectroscopies reveal the catalysis of Ga/ZSM-5 in propane-CO_2 reaction system . In situ XANES and FTIR results suggest that most GaO_x species would be dispersed onto the Brønsted acid sites after H_2 and/or C_3H_8 pretreatment at a high temperature of 550 ℃, resulting in $[GaH_2]^+$ and $[GaH]^{2+}$ species which are the real active sites for propane conversion. In situ CO_2-FTIR experiments of the H_2-pretreated Ga/HZSM-5 indicate that CO_2 can directly reduce gallium hydrides of $[GaH_2]^+$ and $[GaH]^{2+}$ speciesand promote the $[GaH_2]^+$ and $[GaH]^{2+}$ elimination. Therefore, the hydrogen-deficient Ga species can accelerate the C-H bond dissociation and result in new $[GaH_2]^+$ and $[GaH]^{2+}$ species. According to evidences from in situ techniques and $^{13}CO_2$ isotope experiments, we propose the possible reaction networks of the propane-CO_2 coupling reaction including direct propane aromatization, CO_2 hydrogenation, reverse water-gas shift reaction, Boudouard reaction and propane-CO_2 coupling aromatization.

Notes

The authors declare no conflict of interest.

Acknowledgments

This work was supported by the National Key Research and Development Program of China (No. 2022YFE0116000), the National Natural Science Foundation of China (No. 22288101, 21991092, 21991090, 22202193, and 22172166), the Youth Innovation Promotion Association CAS (2021182), the Innovation Research Foundation of Dalian Institute of Chemical Physics, Chinese Academy of Sciences (DICP I202429 and I202217). The authors would like to thank SSRF (BL05U, BL06B and BL14W) beamlines for experimental data collection.

References

[1] Z.-P. Hu, D. Yang, Z. Wang, Z.-Y. Yuan, Chinese J. Catal. 40 (2019) 1233-1254.

[2] P.C.A. Bruijnincx, B.M. Weckhuysen, Angew. Chem. Int. Ed. Engl. 52 (2013) 11980-11987.

[3] X. Ren, Z.-P. Hu, J. Han, Y. Wei, Z. Liu, Front. Chem. Sci. Eng. 17 (2023) 1801-1808.

[4] Y. Ni, W. Zhu, Z. Liu, J. Energy Chem. 54 (2021) 174-178.

[5] K. Yang, J. Li, X. Zhang, Z. Liu, Chinese J. Catal. 39 (2018) 1960-1970.

[6] X. Fang, H. Liu, Z. Chen, Z. Liu, X. Ding, Y. Ni, W. Zhu, Z. Liu, Angew. Chem. Int. Edit. 61 (2022) e202202624.

[7] M. Raad, A. Astafan, S. Hamieh, J. Toufaily, T. Hamieh, J. D. Comparot, C. Canaff, T. J. Daou, J. Patarin, L. Pinard, J. Catal. 365 (2018) 376-390.

[8] M. Xin, E. Xing, X. Gao, Y. Wang, Y. Ouyang, G. Xu, Y. Luo, X. Shu, Ind. Eng. Chem. Res. 58 (2019) 6970-6981.

[9] M.K. Siddiki, J. Li, D. Galipeau, Q. Qiao, Energ. Environ. Sci. 3 (2010) 867-883.

[10] M. G. Sibi, M.K. Khan, D. Verma, W. Yoon, J. Kim, Appl. Catal., B 301 (2022) 120813.

[11] Z. Liu, Y. Ni, T. Sun, W. Zhu, Z. Liu, J. Energy Chem. 54 (2021) 111-117.

[12] M. He, Y. Sun, B. Han, Angew. Chem. Int. Edit. 52 (2013) 9620-9633.

[13] D.E. McCoy, T. Feo, T.A. Harvey, R.O. Prum, Nature Commun. 9 (2018) 1.

[14] P. Zhu, J. Sun, G. Yang, G. Liu, P. Zhang, Y. Yoneyama, N. Tsubaki, Catal. Sci. Technol. 7 (2017) 2695-2699.

[15] Y. Gambo, S. Adamu, G. Tanimu, I.M. Abdullahi, R.A. Lucky, M.S. Ba-Shammakh, M.M. Hossain, Appl. Catal., A 623 (2021) 118273.

[16] X. Jiang, L. Sharma, V. Fung, S.J. Park, C.W. Jones, B.G. Sumpter, J. Baltrusaitis, Z. Wu, ACS Catal. 11 (2021) 2182-2234.

[17] E. Gomez, X. Nie, J.H. Lee, Z. Xie, J.G. Chen, J. Am. Chem. Soc. 141 (2019) 17771-17782.

[18] E. Portillo, J. Gandara-Loe, T.R. Reina, L. Pastor-Pérez, Sci. Total. Environ. 857 (2023) 159394.

[19] C. Wei, J. Li, K. Yang, Q. Yu, S. Zeng, Z. Liu, Chem. Catal. 1 (2021) 1273-1290.

[20] Y. Xu, M. Chen, T. Wang, B. Liu, F. Jiang, X. Liu, J. Catal. 387(2020) 102-118.

[21] Y. Xu, M. Chen, B. Liu, F. Jiang, X. Liu, Chem. Commun. 56 (2020) 4396-4399.

[22] T. Li, T. Shoinkhorova, J. Gascon, J. Ruiz-Martínez, ACS Catal. 11 (2021) 7780-7819.

[23] J. Yang, K. Gong, D. Miao, F. Jiao, X. Pan, X. Meng, F. Xiao, X. Bao, J. Energy Chem. 35 (2019) 44-48.

[24] Y. Song, H. Li, Z. Guo, X. Zhu, S. Liu, X. Niu, L. Xu, Appl. Catal., A 292 (2005) 162-170.

[25] S.J. Han, S.K. Kim, A. Hwang, S. Kim, D.-Y. Hong, G. Kwak, K.-W. Jun, Y.T. Kim, Appl. Catal., B 241 (2019) 305-318.

[26] Z.-P. Hu, J. Han, Y. Wei, Z. Liu, ACS Catal. 12 (2022) 5060-5076.

[27] C. Wei, W. Zhang, K. Yang, X. Bai, S. Xu, J. Li,Z. Liu, Chinese J. Catal. 47 (2023) 138-149.

[28] K. Yang, J. Li, C. Wei, Z. Zhao, Z. Liu, ACS Catal. 13 (2023) 10405-10417.

[29] W. Jung, S. Lee, H. Kim, K. Nam, H.W. Ryu, Y.H. Lim, K.-S. Ha, W.-J. Kim, D.H. Kim, J. Lee, Chem. Eng. J. 450 (2022) 137992.

[30] T. Otroshchenko, G. Jiang, V.A. Kondratenko, U. Rodemerck, E.V. Kondratenko, Chem. Soc. Rev. 50 (2021) 473-527.

[31] H. Fan, X. Nie, C. Song, X. Guo, Ind. Eng. Chem. Res. 61 (2022) 10483-10495.

[32] B. Xu, M. Tan, X. Wu, H. Geng, F. Song, Q. Ma, C. Luan, G. Yang, Y. Tan, Fuel 283 (2021) 118889.

[33] M. Raad, S. Hamieh, J. Toufaily, T. Hamieh, L. Pinard, J. Catal. 366 (2018) 223-236.

[34] M. Yeong Gim, Y. Hyun Lim, K.-Y. Lee, D. Heui Kim, Fuel 304 (2021) 121497.

[35] A. Bhan, W. Nicholas Delgass, Catal. Rev. 50 (2008) 19-151.

[36] X. Niu, X. Nie, C. Yang, J. G. Chen, Catal. Sci. Technol. 10 (2020) 1881-1888.

[37] A. Farsad, S. Lawson, F. Rezaei, A.A. Rownaghi, Catal. Today 374 (2021) 173-184.

[38] A. Caiola, B. Robinson, S. Brown, X. Wang, Y. Wang, J. Hu, Catal. Commun. 176 (2023) 106631.

[39] J.S. Espindola, C.J. Gilbert, O.W. Perez-Lopez, J.O. Trierweiler, G.W. Huber, Fuel Process. Technol. 201 (2020) 106319.

[40] Z. Ni, Y. Li, Y. Zhang, Y. Wang, G. Cui, G. Jiang, Z. Zhao, C. Xu, Chem. Eng. Sci. 245(2021) 116856.

[41] S. Majhi, K.K. Pant, J. Ind. Eng. Chem. 20 (2014), 2364-2369.

[42] F. Magzoub, X. Li, J. Al-Darwish, F. Rezaei, A.A. Rownaghi, Appl. Catal., B 245 (2019) 486-495.

[43] C. Bi, Z. Zhang, D. Han, C. Wang, J. Zhang, M. Sun, Q. Hao, H. Chen, X. Ma, Fuel 321 (2022) 124105.

[44] Y. Yuan, C. Brady, L. Annamalai, R.F. Lobo, B. Xu, J. Catal. 393(2021) 60-69.

[45] Y. Yuan, R.F. Lobo, B. Xu, ACS Catal. 12 (2022) 1775-1783.

[46] Y. Yuan, C. Brady, R.F. Lobo, B. Xu, ACS Catal. 11 (2021), 10647-10659.

[47] V.d.O. Rodrigues, A.C. Faro Júnior, Appl. Catal., A 435-436 (2012) 68-77.

[48] B.W.L. Southward, R.J. Nash, C.T. O'Connor, Appl. Catal., A 135 (1996) 177-191.

[49] Y. Yuan, Z. Zhao, R.F. Lobo, B. Xu, Adv. Sci. 10 (2023) 2207756.

[50] S. Bordiga, E. Groppo, G. Agostini, J.A. van Bokhoven, C. Lamberti, Chem. Rev. 113 (2013) 1736-1850.

[51] A. Jia, W. Zhang, H. Peng, Y. Zhang, T. Song, L. Li, Y. Ye, Y. Wang, M. Luo, D.-L. Chen, W. Huang, J.-Q. Lu, J. Catal. 425 (2023) 57-69.

[52] H. Kim, J. Kim, J.H. Kwak, J. Phys. Chem. C 127 (2023) 7142-7150.

[53] M. Roiaz, L. Falivene, C. Rameshan, L. Cavallo, S.M. Kozlov, G. Rupprechter, J. Phys. Chem. C 123 (2019) 8112-8121.

[54] G.L. Price, E. Iglesia, Ind. Eng. Chem. Res. 28 (1989) 839-844.

[55] C. Wei, Q. Yu, J. Li, Z. Liu, ACS Catal. 10 (2020) 4171-4180.

Graphical abstract

In situ FTIR and XANES analyses elucidate the dynamic gallium hydride species under working conditions, serving as the active sites for propane-CO_2 coupling conversion to aromatics and syngas.

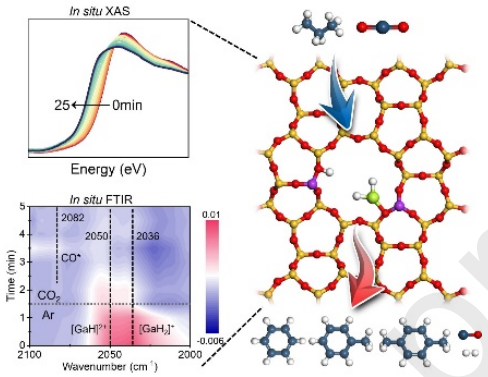

The authors declare no conflict of interest.